Hindawi
Mathematical Problems in Engineering
Volume 2022, Article ID 9485634, 7 pages
https://doi.org/10.1155/2022/9485634

Research Article

Meshing Characteristics of Toroidal Drive of Spherical Planetary Gear

Yanhua Zhang and Jujiang Cao

College of Mechanical & Engineering, Shaanxi University of Science and Technology, Xi'an 710021, China

Correspondence should be addressed to Yanhua Zhang; zhangyanhua@sust.edu.cn

Received 25 February 2022; Accepted 2 April 2022; Published 14 May 2022

Academic Editor: Zaoli Yang

Globoidal cam transmission of planetary gear train is a complex form of space transmission. The curved surface and meshing state of the inner and outer globoidal cam are determined by the curved surface of the rolling tooth on the planetary gear. Therefore, a unified mathematical expression method of the curved surface of the rolling tooth of the planetary gear is established. The envelope of the contact line on the tooth surface of the inner and outer cambered cam is a kind of boundary line, which determines the undercut limit of this kind of transmission, and the second kind of boundary line determines the meshing limit of this kind of transmission. Based on the principle of spatial meshing, the contact line between the curved surface of the rolling tooth on the planetary gear and the inner and outer globoidal cam is deduced, and the tooth profile curved surface equation of the spherical tooth and the inner and outer globoidal cam is analyzed. The boundary curve equation of planetary gear with spherical teeth is studied. By comparing transmission parameters of a/R, i_1^H, i_2^H, β, and $\triangle\beta$, the influence of transmission parameters on the meshing characteristics of globoidal cam transmission of planetary gear train is analyzed. The research in this paper is helpful to realizing the manufacture of a prototype.

1. Introduction

Globoidal cam transmission mechanism of planetary gear train is a new type of composite transmission mechanism, also known as toroidal drive. The meshing principle of the mechanism is essentially the meshing principle of globoidal cam, and it is studied from the perspective of globoidal cam. Toroidal drive combines the planetary transmission and spatial globoidal cam transmission, which has the characteristics of both the transmissions. The meshing form from sliding to rolling is realized, and it has the advantages of compact structure, large transmission ratio, and high transmission efficiency [1–4]. The design, manufacture, and test of this transmission mechanism are all researched by the scholars. The calculation formula of contact stress between planet and worm or ring internal gear is deduced. The calculation method of contact strength of toroidal transmission is given [5]. The analytical relationship among the output torque of multitooth engagement is deduced. The fluctuation of the output torque is analyzed and calculated [6]. The meshing equation of the toroidal drive with cylindrical tooth is established by using space meshing theory, and the calculation formulas of pressure angle of the planet worm gear and the toroidal internal gear are also given [7]. In this method, the phase error optimization is realized by the angle precise rotation matching of the actual lift data. Also, compared with the precision of high-precision measuring equipment, the method can extract the lift and phase angle error of the cam accurately and stably [8]. The reverse program of motion law of spherical indexing cam mechanism is developed, and the method of solving the motion law of driven plate with reverse design idea is described. The parametric modeling of spherical indexing cam is realized by using UG [9]. Nguyen et al. [10] presented the modeling, controller design, and testing of the integrated permanent magnet toroidal motor drive. As one kind of direct-drive composite motor drive, the integration and configuration for permanent magnet toroidal motor are presented. The

dynamic machine model for permanent magnet toroidal motor drive is established with nonlinear time-varying electromagnetic parameters, which include inductances and differential information. A general framework for motion design of the follower in cam mechanisms by using non-uniform rational B-spline is proposed in order to facilitate the modeling of the mechanism [11].

Therefore, a lot of studies about the toroidal drive were done which include design theories and manufacturing techniques. However, the unified mathematical expression method of the rolling tooth surface of the planetary gear is not established. Here, the contact line equation between the rolling tooth surface and the inner and outer cambered cam on the planetary gear is deduced based on the spatial meshing principle. The tooth profile surface equation of the spherical tooth and the inner and outer cambered cam is analyzed. The boundary curve equation of planetary gear with spherical teeth is studied. By introducing transmission parameters, the influence of transmission parameters on the meshing characteristics of globoidal cam transmission of planetary gear train is analyzed.

2. Transmission Principle of Toroidal Drive

Toroidal drive is a complex spatial meshing driving mechanism, as shown in Figure 1, which consists of inner globoidal cam, outer globoidal cam, planetary wheel, and planetary frame.

The planetary wheels are evenly distributed around the axis of the inner globoidal cam, which mesh with the inner and outer globoidal cams simultaneously. The planetary wheels are the transmission components of the power of the mechanism, and the wheel teeth on them may be rolling balls, rollers, or rolling cones. The rotation motion is input by the outer globoidal cam to drive the planetary wheel which is fixed to the planetary frame to rotate. Also, the output of the motion is realized.

2.1. Establishment of a Unified Mathematical Expression for the Surface of Revolution. Although there are many different types of planetary gear teeth of the toroidal drive, their curved surface shape is rotary curved surface. Let the front view of the projection of this revolving surface on the o-xyz plane be as shown in Figure 2. The surface is formed by the rotation of plane curve C-C around the x-axis, and curve C-C is the generatrix of the surface. Generally, the busbar C-C is composed of a circular arc, and the chord of the circular arc is parallel to the connecting line between the large and small ends of the rotating body. In the xoy plane, the distance between the instantaneous contact point K on the left bus C-C and the large end of the rotating body is d. Its coordinate is K (δ , - rf+ $\delta \tan \gamma$). The circle center O of the circular arc of the rotating body bus is on the straight line ko' passing K perpendicular to C-C. Let the coordinates of the center o' of the bus arc be o'(X_{of}, Y_{of}) and the radius be r_a. It can be seen that the revolving equation iswhere δ represent the surface parameters of revolution.

$$y_f + \left(r_f - \delta_f \tan \gamma\right) = \tan \gamma \left(x_f - \delta_f\right), \tag{1}$$

The equation of ko' is

$$y_f + \left(r_f - \delta \tan \gamma\right) = -\tan \gamma \left(x_f - \delta\right). \tag{2}$$

The distance between two points (k, O′) is

$$\left(X_{of} - \delta\right)^2 + \left(Y_{of} + \delta\left(r_f - \delta \tan \gamma\right)\right)^2 = r_a^2. \tag{3}$$

While the distance between the rotating body is δ_f, the truncated radius r_f' is

$$r_f{}' = \sqrt{r_a^2 - \left(\delta_f - \delta + ra \sin \gamma\right)^2} - r_a \cos \gamma + \left(r_f - \delta \tan \gamma\right). \tag{4}$$

The surface equation of the body of revolution is

$$R_f = \begin{Bmatrix} x_f \\ y_f \\ z_f \end{Bmatrix} = \begin{Bmatrix} \delta_f \\ \left(\sqrt{r_a^2 - \left(\delta_f - \delta + ra \sin \gamma\right)^2} - r_a \cos \gamma + \left(r_f - \delta \tan \gamma\right)\right)\cos \beta_f \\ \left(\sqrt{r_a^2 - \left(\delta_f - \delta + ra \sin \gamma\right)^2} - r_a \cos \gamma + \left(r_f - \delta \tan \gamma\right)\right)\sin \beta_f \end{Bmatrix}, \tag{5}$$

where there are different forms of surface of revolution equations when γ and r_a have different values.

2.2. Tooth Profile Surface Equation of Inner and Outer Globoidal Cams under Circular Tooth. In the globoidal cam transmission of planetary gear train, the radius of planetary gear is set as R, z planetary gear teeth composed of rotating surface are evenly distributed on it, and the center distance from outer globoidal cam to planetary gear is a. In order to find the meshing equation, the coordinate system shown in Figure 3 is set.

The fixed coordinate system O_0-$X_0Y_0Z_0$ is fixedly connected with the inner arc cam. The dynamic coordinate system O_1-$X_1Y_1Z_1$ is fixedly connected with the outer cambered cam. The dynamic coordinate system O_H-

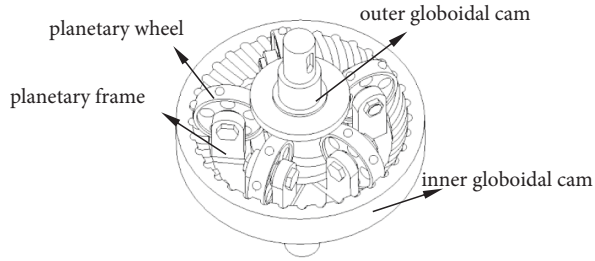

Figure 1: Toroidal drive.

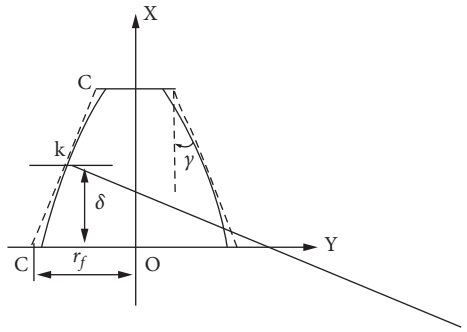

Figure 2: Coordinate system of revolving surface.

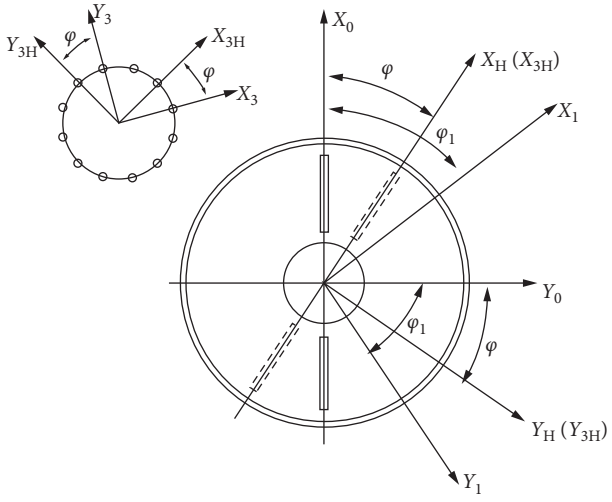

Figure 3: Setting of coordinate system.

$X_HY_HZ_H$ is fixedly connected with the planet carrier. O_0Z_0, O_1Z_1, and O_HZ_H shafts have the same direction as the outer cambered cam axis. The dynamic coordinate system O_{3H}-$X_{3H}Y_{3H}Z_{3H}$ is fixedly connected with the planet carrier. O_3-$X_3Y_3Z_3$ is fixedly connected with the planetary gear. The direction of $O_{3H}Z_{3H}$ axis and O_3-Z_3 axis is the same as that of planetary axis.

When $r_a = r_f = r$, $\gamma = 45^\circ$, the instantaneous meshing point K of the rolling teeth of the planetary gear is at the root of the rotary body. And K is the distance from the big end of the revolving surface, $\delta = 0$. At this time, the surface of revolution is a sphere. The surface equation of the rotating body is

$$R_f^{(f)} = \begin{bmatrix} R + r\cos\theta\sin\phi \\ r\cos\theta\sin\phi \\ r\sin\theta \end{bmatrix}. \quad (6)$$

The tooth surface equation of outer globoidal cam is

$$\begin{cases} R_1^{(f)} = \begin{bmatrix} (R\cos\phi + r\cos\theta\cos(\varphi+\phi)+a)\cos(\phi_H-\phi_1) - r\sin\theta\sin(\phi_H-\phi_1) \\ (R\cos\phi + r\cos\theta\cos(\varphi+\phi)+a)\sin(\phi_H-\phi_1) + r\sin\theta\cos(\phi_H-\phi_1) \\ R\sin\phi + r\cos\theta\sin(\varphi+\phi) \end{bmatrix}, \\ \tan\theta = -\dfrac{1}{i_1^H}\dfrac{\sin\varphi}{a/R+\cos\phi}. \end{cases} \tag{7}$$

The tooth surface equation of inner globoidal cam is

$$\begin{cases} R_2^{(f)} = \begin{bmatrix} (R\cos\phi + r\cos\theta\cos(\varphi+\phi)+a)\cos\phi_H - r\sin\theta\sin\phi_H \\ (R\cos\phi + r\cos\theta\cos(\varphi+\phi)+a)\sin\phi_H + r\sin\theta\cos\phi_H \\ R\sin\phi + r\cos\theta\sin(\varphi+\phi) \end{bmatrix}, \\ \tan\theta = -\dfrac{1}{i_2^H}\sin\varphi/\dfrac{a}{R}+\cos\phi. \end{cases} \tag{8}$$

2.3. Solution of Lower Limit Curve of Spherical Tooth. The envelope of the contact line on the tooth surface of the inner and outer cambered cam is a kind of boundary line, which determines the undercut limit of this kind of transmission, and the second kind of boundary line determines the meshing limit of this kind of transmission. Next, the boundary curve of this kind of transmission form is solved and analyzed. According to the meshing theory, the calculation formula of a bound function is

$$\Psi = \frac{1}{D^2}\begin{vmatrix} E & F & r_u^{(f)}V_{12} \\ F & G & r_v^{(f)}V_{12} \\ \varphi_u & \varphi_v & \varphi_t \end{vmatrix}, \tag{9}$$

where $E = (r_u^{(f)})^2$; $F = r_u r_v$; $G = (r_v)^2$; and $D = EG - F^2$.

According to the meshing theory, the calculation formula of the second bound function is

$$\varphi(u, v, t) = 0. \tag{10}$$

The above formula can be used to obtain a boundary curve equation when the spherical teeth of the planetary gear teeth mesh with the outer and inner globoidal cams:

$$\begin{cases} R_1^{(f)} = \begin{bmatrix} (R\cos\phi + r\cos\theta\cos(\varphi+\phi)+a)\cos(\phi_H-\phi_1) - r\sin\theta\sin(\phi_H-\phi_1) \\ (R\cos\phi + r\cos\theta\cos(\varphi+\phi)+a)\sin(\phi_H-\phi_1) + r\sin\theta\cos(\phi_H-\phi_1) \\ R\sin\phi + r\cos\theta\sin(\varphi+\phi) \end{bmatrix}, \\ \tan\theta = -\dfrac{1}{i_1^H}\dfrac{\sin\varphi}{(a/R)+\cos\phi}, \\ \Psi = 0, \end{cases}$$

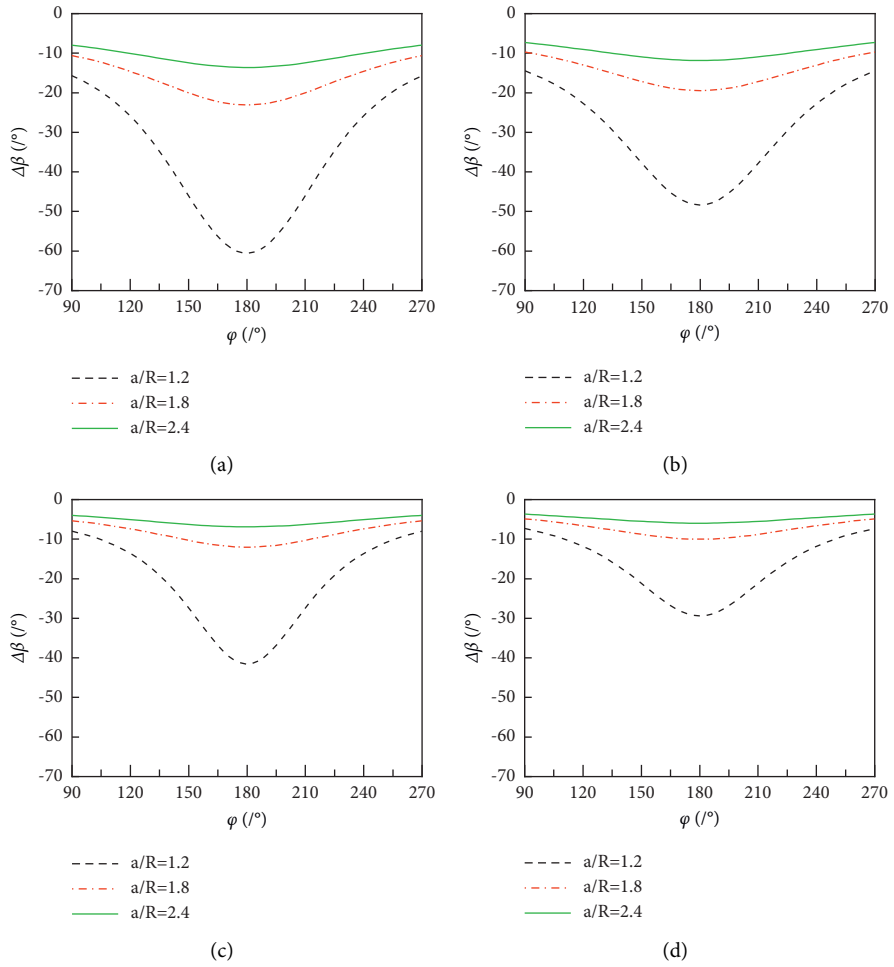

FIGURE 4: The change of β when the cylinder of planetary gear teeth is meshed with the cam of outer cambered surface. (a) $i_1^H = 3$. (b) $i_1^H = 5$. (c) $i_1^H = 6$. (d) $i_1^H = 8$.

$$\begin{cases} R_2^{(f)} = \begin{bmatrix} (R\cos\phi + r\cos\theta\cos(\varphi+\phi) + a)\cos\phi_H - r\sin\theta\sin\phi_H \\ (R\cos\phi + r\cos\theta\cos(\varphi+\phi) + a)\sin\phi_H + r\sin\theta\cos\phi_H \\ R\sin\phi + r\cos\theta\sin(\varphi+\phi) \end{bmatrix}, \\ \tan\theta = -\dfrac{1}{i_2^H}\dfrac{\sin\varphi}{a/R + \cos\phi}, \\ \Psi = 0, \end{cases} \tag{11}$$

where $\varphi_u = i(a/R + \cos\phi)/\cos^2\phi$, and

$$\begin{aligned} \varphi_v &= \cos\phi, \\ \varphi_t &= -i\sin\phi\tan\theta, \\ r_u^{(f)}V_{12} &= -ir^2\cos(\varphi+\phi) + ir\cos\theta(a + R\cos\phi) \\ &\quad - Rr\sin\theta\sin\phi, \\ r_v^{(f)}V_{12} &= -ir^2\sin\theta\cos\theta\sin(\varphi+\phi) \\ &\quad + r^2\cos^2\theta + Rr\sin\theta\cos\phi. \end{aligned} \tag{12}$$

By solving the first kind of boundary curve equation under the shape of upper spherical tooth, it is known that there is no solution to the equation. It shows that there is no undercutting on the tooth surfaces of inner and outer globoidal cams in the globoidal cam transmission mechanism of planetary gear system under the tooth shape of star gear planetary gear.

By solving the equation of the second kind of boundary curve under the tooth shape of the upper spherical planetary gear, it is known that the second kind of boundary curve

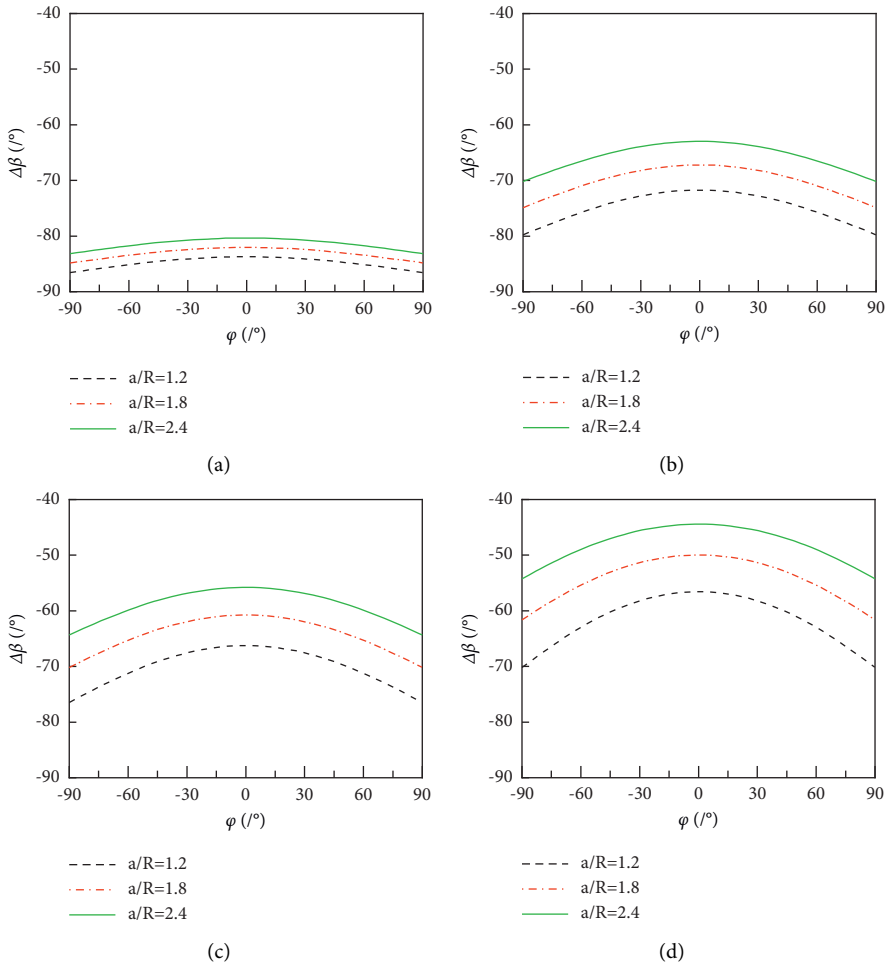

FIGURE 5: The change of β when the cylinder of planetary gear teeth is meshed with the cam of inner cambered surface. (a) $i_2^H = 0.05$. (b) $i_2^H = 0.15$. (c) $i_2^H = 0.2$. (d) $i_2^H = 0.3$.

degenerates into the vertex of a sphere. At this point, $\theta = 0$ and $\varphi = 0$. It can be seen that the contact lines between the planetary gear and the inner and outer cambered cam pass through the spherical apex.

3. Meshing Zone Analysis

The contact line on the spherical tooth surface is

$$\frac{y}{z} = \frac{\sin\varphi}{\tan\beta} = -i\left(\frac{a}{R} + \cos\phi\right),$$
$$\tan\beta = -\frac{1}{i(a/R + \cos\phi)}. \tag{13}$$

It can be seen that the contact line between the ball tooth and the inner and outer cambered cam is a plane arc passing through the apex of the ball, and the radius of the arc is equal to the radius of the ball. In theory, the length of the contact line is equal to a quarter of the plane arc. Use the included angle between the plane where the contact line is located and the plane where xoy is located β. It can reflect the distribution of the contact area, which can be obtained from the geometric relationship shown in the figure. It can be seen from the above formulas (13) and (14), when i and a/R are fixed values, the change of the planetary gear φ will be lead to β fluctuation within a certain range $\triangle\beta$. β can reflect the position of the contact area, and $\triangle\beta$ reflects the size of the contact area. When the ball gear contacts the outer and inner cambered cams, the size and position of its contact area with the parameters i and a/R are shown in Figures 4 and 5.

From Figure 4, when φ are 180° and 90° (or 270°), respectively, β are the maximum and minimum of their absolute values, respectively, indicating that the contact line is the farthest and closest to xoy plane, respectively. With the increase of a/R and i_1^H, $\beta$and $\triangle\beta$ decrease rapidly, which shows that the contact area decreases rapidly with the rapid approach of the contact area to the xoy plane.

From Figure 5, when the angle is 0° and ±90°, respectively, β is the minimum and maximum of its absolute value, respectively, and the contact line is the closest and farthest from xoy plane, respectively. With the increase of parameter a/R, β and $\triangle\beta$ decrease, which indicates that the contact area approaches the plane where xoy is located. The contact area decreased at the same time, but the decrease is not obvious. With the increase of i_2^H, β and $\triangle\beta$ increased, which indicates that the contact area will increase significantly when it is

close to the plane where xoy is located. It also shows that in this case, the impact i_2^H is more obvious than that of a/R.

4. Conclusion

To summarize, a unified mathematical model of planetary gear tooth types is established, and on this basis, a parameterized unified meshing equation of globoidal cam transmission of planetary gear train is established. Based on the above equation, the tooth profile surface equation of inner and outer globoidal cams under the typical planetary tooth shape of ball is deduced. The influence law of transmission parameters on meshing area is analyzed. Through the study of this paper, it indicated that the transmission ratio i is followed by the radius of planetary wheel R, the center distance a, and the radius of spherical tooth successively. And the research is helpful to realizing the manufacture of a prototype.

Data Availability

The data used in this paper are based on theoretical calculation and analysis.

Conflicts of Interest

The authors declare that they have no conflicts of interest.

Acknowledgments

This study was supported by Natural Science Foundation of Shaanxi Education Department of China (no. 18JK0119).

References

[1] M. Müller, M. Hoffmann, M. Hüsing, and B. Corves, "Using servo-drives to optimize the transmission angle of cam mechanisms," *Mechanism and Machine Theory*, vol. 135, no. 2, pp. 165–175, 2019.

[2] J. Dong, X. Weng, and K. Wang, "The new progress of the worm transmission Technology in China," *Machine Design and Manufacturing Engineering*, vol. 43, no. 4, pp. 78–81, 2016.

[3] L. Xu and L. Fu, "Toroidal drive with half stator," *Advances in Mechanical Engineering*, vol. 7, no. 6, pp. 8132–8140, 2015.

[4] L. S. Yousuf, "Nonlinear dynamics phenomena in globoidal cam with roller follower mechanism," *Chaos, Solitons & Fractals*, vol. 150, no. C, pp. 111–132, 2021.

[5] S. P. Yang, Y. Q. Tan, Y. L. Pan, L. M. Li, and J. G. Liu, "Contact strength of toroidal drive with cylindrical teeth," *Applied Mechanics and Materials*, vol. 288, pp. 92–97, 2013.

[6] X. Liu and H. Wang, "Analysis on torque ripple characteristics for toroidal electromechanical drive," *Mechanical Science and Technology for Aerospace Engineering*, vol. 37, no. 6, pp. 867–872, 2019.

[7] B. Liu, J. Cao, and Y. Zhang, "Modeling of globoidal cam planetary mechanism by simulating motion method," *Journal of Mechanical Transmission*, vol. 42, no. 1, pp. 33–36, 2018.

[8] Y. Liu, P. Chen, J. Ding et al., "Extraction methods and implementation technologies of fuel injection pump cam profile characteristics," *Mathematical Problems in Engineering*, vol. 2021, pp. 1–7, Article ID 6657632, 2021.

[9] Y. Shi, "Research on computer aided design and machining of equipment globoidal cam," *Journal of Physics: Conference Series*, vol. 1648, no. 3, pp. 132–168, 2020.

[10] T. T. N. Nguyen, S. Kurtenbach, M. Hüsing, and B. Corves, "A general framework for motion design of the follower in cam mechanisms by using non-uniform rational B-spline," *Mechanism and Machine Theory*, vol. 137, no. 3, pp. 374–385, 2019.

[11] X. Liu, D. Li, and L. Zuo, "Modeling and control for an integrated permanent magnet toroidal motor drive with nonlinear electromagnetic parameters," *Applied Mathematical Modelling*, vol. 89, no. 1, pp. 154–170, 2021.